

1 **A plant pathogen utilizes effector proteins for microbiome manipulation**

2

3 Nick C. Snelders<sup>1</sup>, Hanna Rovenich<sup>1,#</sup>, Gabriella C. Petti<sup>1,2,#</sup>, Mercedes Rocafort<sup>1,‡</sup>, Julia A. Vorholt<sup>2</sup>,

4 Jeroen R. Mesters<sup>3</sup>, Michael F. Seidl<sup>1,4</sup>, Reindert Nijland<sup>1,§</sup>, Bart P.H.J. Thomma<sup>1,5,\*</sup>

5

6 <sup>1</sup>Laboratory of Phytopathology, Wageningen University & Research, Wageningen, The Netherlands

7 <sup>2</sup>Institute of Microbiology, ETH Zürich, Zürich, Switzerland

8 <sup>3</sup>Institute of Biochemistry, University of Lübeck, Center for Structural and Cell Biology in Medicine,

9 Lübeck, Germany

10 <sup>4</sup>Theoretical Biology & Bioinformatics Group, Department of Biology, Utrecht University, Utrecht, The

11 Netherlands

12 <sup>5</sup>Cluster of Excellence on Plant Sciences (CEPLAS), University of Cologne, Botanical Institute, Cologne,

13 Germany

14

15 <sup>#</sup>These authors contributed equally

16 <sup>‡</sup>Current address: School of Agriculture and Environment, Massey University, Palmerston North, New

17 Zealand

18 <sup>§</sup>Current address: Marine Animal Ecology Group, Wageningen University & Research, Wageningen,

19 The Netherlands

20 <sup>\*</sup>Corresponding author. Email: [bart.thomma@wur.nl](mailto:bart.thomma@wur.nl)

## 21 **Abstract**

22 **During colonization of their hosts, pathogens secrete effector proteins to promote disease**  
23 **development through various mechanisms. Increasing evidence shows that the host microbiome**  
24 **plays a crucial role in health, and that hosts actively shape their microbiomes to suppress disease.**  
25 **We hypothesized that pathogens evolved to manipulate host microbiomes to their advantage in**  
26 **turn. Here, we show that the fungal plant pathogen *Verticillium dahliae* utilizes effector proteins**  
27 **for niche colonization through selective manipulation of host microbiomes by suppressing**  
28 **microbes with antagonistic activities. Moreover, we show that effector proteins are similarly**  
29 **exploited for microbiome manipulation in the soil environment, where the fungus resides in**  
30 **absence of a host. In conclusion, we demonstrate that pathogens utilize effector proteins to**  
31 **modulate microbiome compositions and propose that their effector catalogs represent an**  
32 **untapped resource for novel antibiotics.**

33

## 34 **Introduction**

35 To establish disease, pathogenic microbes secrete a wide diversity of effector proteins that facilitate  
36 host colonization through a multitude of mechanisms<sup>1</sup>. Typically, pathogen effectors are defined as  
37 small cysteine-rich proteins that are secreted upon colonization to manipulate host physiology or to  
38 deregulate host immune responses<sup>2</sup>. Consequently, effector proteins are predominantly studied in  
39 binary host-microbe interactions, while largely ignoring the biotic context in which these interactions  
40 take place. Higher organisms, including plants, associate with a plethora of microbes that collectively  
41 form their microbiome, which represents a key determinant for their health<sup>3-7</sup>. The most extensive  
42 microbial colonization of plants occurs at roots, where plants define rhizosphere microbiome  
43 compositions through secretion of exudates<sup>8,9</sup> and specifically attract beneficial microbes to suppress  
44 pathogen invasion<sup>10-12</sup>. Thus, we hypothesized that plant pathogens evolved mechanisms to  
45 counteract this recruitment and modulate host microbiomes for successful infection, possibly  
46 through effector proteins<sup>1,13</sup>.

47 *Verticillium dahliae* is a soil-borne fungus that causes vascular wilt disease on hundreds of plant  
48 species, including numerous crops<sup>14,15</sup>. *V. dahliae* survives in the soil through persistent resting  
49 structures called microsclerotia that germinate in response to nutrient-rich exudates released by  
50 nearby plant roots<sup>16</sup>. Subsequently, emerging hyphae grow through the soil and rhizosphere towards  
51 the roots where the fungus penetrates its hosts. Following root penetration, *V. dahliae* invades the  
52 xylem where it produces conidiospores that are spread throughout the vasculature by the sap  
53 stream. This systemic colonization causes chlorosis and necrosis of plant tissues, which is followed by  
54 plant senescence. *V. dahliae* then enters a saprophytic phase, emerges from the vasculature and  
55 colonizes the dead plant material where it produces new microsclerotia that are eventually released  
56 into the soil upon tissue decomposition.

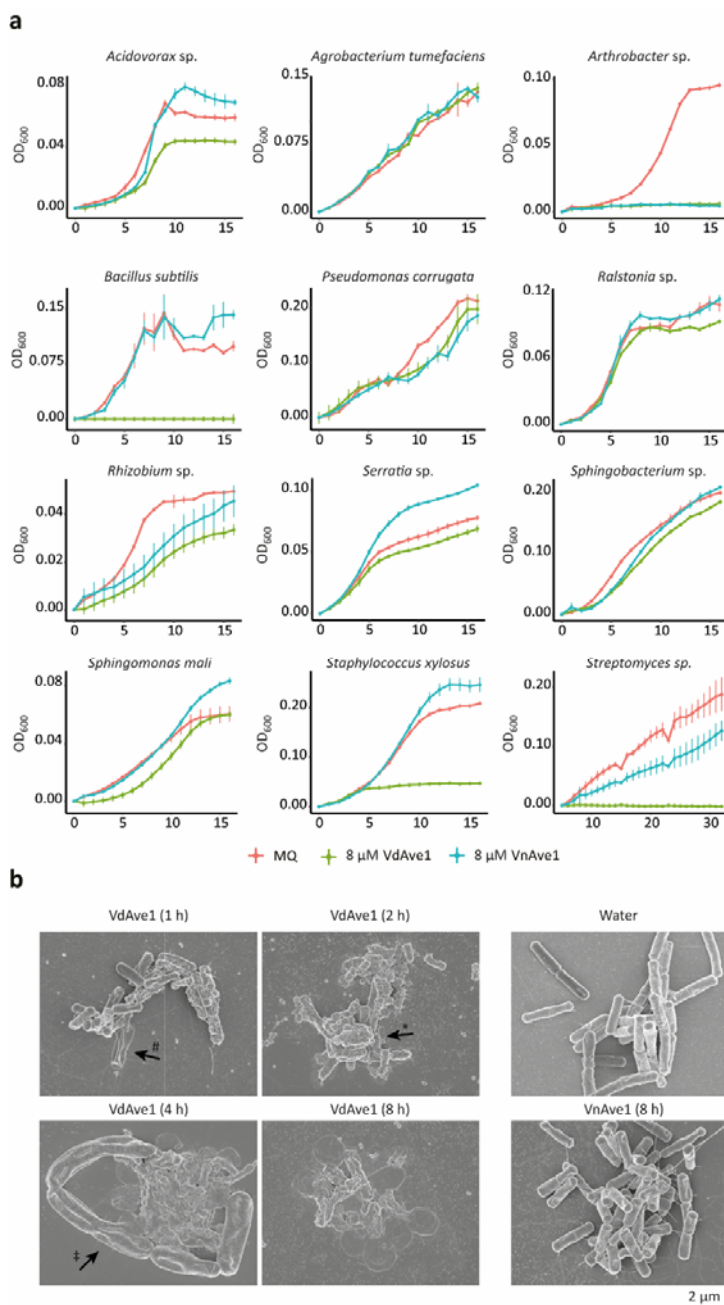
57 Using comparative population genomics, we previously identified the *V. dahliae*-secreted small  
58 cysteine-rich effector protein Ave1 that is recognized as an avirulence determinant by tomato plants  
59 that carry the corresponding Ve1 immune receptor<sup>17</sup>. However, on host plants lacking Ve1, VdAve1  
60 acts as a virulence effector that promotes fungal colonization and disease development<sup>17</sup>.  
61 Interestingly, VdAve1 is homologous to plant natriuretic peptides (PNPs) that have been identified in  
62 numerous plant species, suggesting that *VdAve1* was acquired from plants through horizontal gene  
63 transfer<sup>17</sup>. Whereas several of the plant PNPs were shown to act in plant homeostasis and (a)biotic  
64 stress responses<sup>18,19</sup>, the mode of action of VdAve1 to contribute to fungal virulence has remained  
65 unknown.

66 Intriguingly, unlike most pathogen effector genes characterized to date, *VdAve1* is not only highly  
67 expressed during host colonization<sup>17,20</sup>, but also during growth *in vitro* and under conditions  
68 mimicking soil colonization, suggesting a ubiquitous role throughout the fungal life cycle including life  
69 stages outside the host, and thus a role that does not primarily involve targeting host plant  
70 physiology (Extended data Fig. 1). Our attempts to purify VdAve1 upon heterologous expression in  
71 *Escherichia coli*, to facilitate functional characterization, repeatedly failed due to the formation of

72 inclusion bodies (Extended data Fig. 2a). The inability to obtain soluble protein using heterologous  
73 microbial expression systems can be attributed to a multitude of reasons, but is a well-known  
74 phenomenon when expressing antimicrobial proteins<sup>21</sup>. Consequently, based on the ubiquitous  
75 expression of *VdAve1* by *V. dahliae*, and our inability to purify soluble *VdAve1* following expression in  
76 *E. coli*, we hypothesized that *VdAve1* may possess antimicrobial activity.

77 To obtain functional *VdAve1*, inclusion bodies were isolated from *E. coli* cells and denatured using  
78 guanidine hydrochloride. Next, *VdAve1* was refolded by stepwise dialysis and functionality was  
79 confirmed through testing recognition by its immune receptor *Ve1* (Extended data Fig. 2b). To assess  
80 the potential antimicrobial activity of *VdAve1*, we developed an *in vitro* system in which we  
81 incubated a panel of plant-associated bacteria in tomato xylem fluid, to mimic a natural environment  
82 in which *VdAve1* is secreted, namely tomato xylem vessels, and monitored their growth in presence  
83 and absence of the protein. Interestingly, *VdAve1* selectively inhibited the growth of plant-associated  
84 bacteria (Fig. 1a). Whereas growth of all Gram positive bacteria tested, namely *Arthrobacter* sp.,  
85 *Bacillus subtilis*, *Staphylococcus xylosus* and *Streptomyces* sp., was strongly inhibited, Gram negative  
86 bacteria displayed differential sensitivity to the protein. Intriguingly, this differential sensitivity is not  
87 immediately explained by phylogenetic relationships of the tested isolates as even within bacterial  
88 orders/families differences are observed. For instance, whereas growth of the burkholderiales  
89 species *Acidovorax* is inhibited by *VdAve1*, growth of a *Ralstonia* isolate, which belongs the same  
90 order, is not. Similarly, treatment of two closely related rhizobiales, *Rhizobium* sp. and  
91 *Agrobacterium tumefaciens*, revealed differential sensitivity as *VdAve1* affected growth of *Rhizobium*  
92 sp., but not of *A. tumefaciens*. Finally, growth of *Pseudomonas corrugata* and *Serratia* sp. was only  
93 slightly altered and unaffected, respectively, while growth of both *Sphingobacterium* sp. and  
94 *Sphingomonas mali* was affected upon exposure to *VdAve1*. Interestingly, growth of the endophytic  
95 fungus *Fusarium oxysporum* and the fungal mycoparasite *Trichoderma viride* was not inhibited by  
96 *VdAve1*, suggesting that *VdAve1* exerts antibacterial, but not antifungal, activity (Extended data Fig.

97 3a). These initial observations with divergent, randomly chosen, plant-associated bacteria prompted  
 98 us to further characterize the antimicrobial activity of VdAve1.



99

100 **Fig. 1: Bactericidal activity of *Verticillium dahliae* effector VdAve1.** **a**, VdAve1 selectively inhibits *in*  
 101 *vitro* growth of plant-associated bacterial isolates in tomato xylem fluid. The close homolog VnAve1  
 102 from *V. nubilum* only inhibits a subset of the bacteria affected by VdAve1 and is generally less  
 103 effective. **b**, Scanning electron microscopy of *B. subtilis* upon 1, 2, 4 and 8 hours of incubation in  
 104 tomato xylem fluid showing blebbing (\*), swelling (‡) and lysis (#) with 6.5  $\mu$ M VdAve1 (0.8 x MIC),  
 105 but not with water or VnAve1.

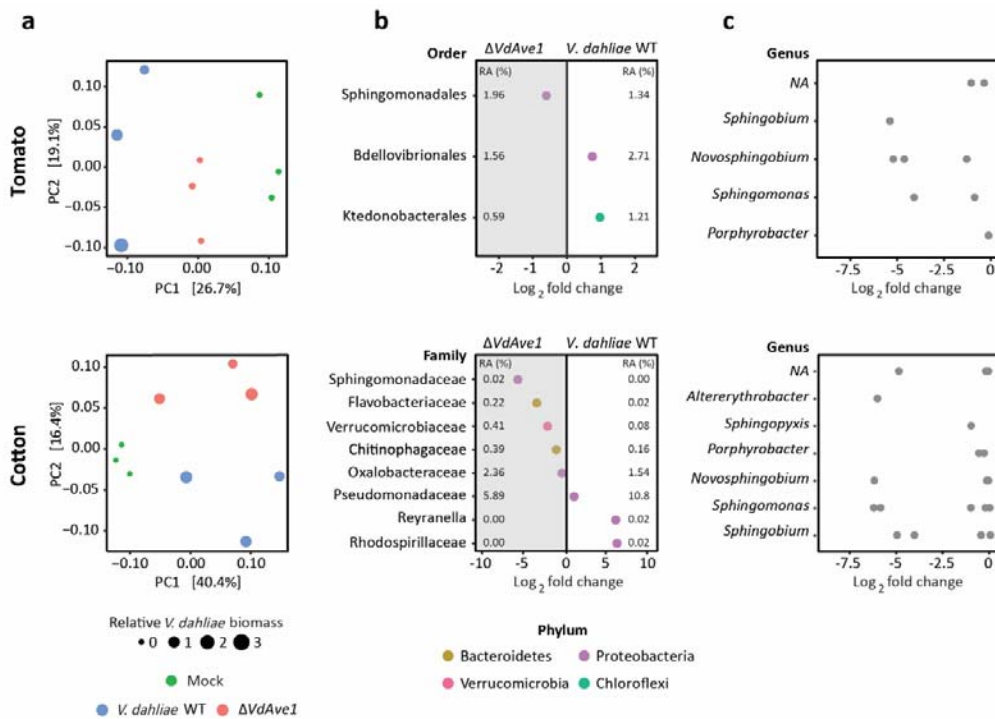
106 As a first step in the further characterization of the antimicrobial activity of VdAve1, we aimed to  
107 determine whether the effector protein is bacteriostatic or bactericidal by making use of electron  
108 microscopy to visualize the effect of protein treatment on bacteria. As a target species the Gram  
109 positive *B. subtilis* was chosen, considering its high sensitivity to VdAve1 treatment. By testing a  
110 concentration series of the VdAve1 effector protein, the minimum inhibitory concentration (MIC)  
111 was determined at 8  $\mu$ M (Extended data Fig. 3b). However, electron microscopy analysis revealed  
112 that sub-MIC concentrations of VdAve1 already induced blebbing and swelling of bacterial cells,  
113 followed by lysis and collapse, corresponding with bactericidal activity (Fig. 1b).

114 To investigate whether the antimicrobial activity that is displayed by VdAve1 is more widely  
115 conserved among its homologs, we tested the only homolog that occurs in one of the sister species  
116 of the *Verticillium* genus, namely VnAve1, from the non-pathogenic species *V. nubilum* that displays  
117 90% amino acid identity (Extended data Fig. 3c). Interestingly, also this homolog displays  
118 antimicrobial activity, albeit that it only inhibits a subset of the bacteria affected by VdAve1, and  
119 does not cause *B. subtilis* lysis (Fig. 1). Thus, the 13 amino acid polymorphisms between the two Ave1  
120 homologs are responsible for differences in the activity spectrum. To investigate whether the  
121 antimicrobial activity also occurs among plant homologs, or is confined to microbial homologs and  
122 involves neofunctionalization after horizontal transfer, the more distant homolog AtPNP-A from  
123 *Arabidopsis thaliana* was tested as well. Intriguingly, AtPNP-A completely arrests *B. subtilis* growth  
124 (Extended data Fig. 3c,d). Collectively, these findings demonstrate that various Ave1 homologs  
125 possess antimicrobial activity, yet with divergent activity spectra, and suggest that the antimicrobial  
126 activity of VdAve1 did not result from neofunctionalization following horizontal gene transfer.

127 Based on the strong but selective bactericidal activity of VdAve1 *in vitro*, we hypothesized that *V.*  
128 *dahliae* exploits its effector protein to affect host microbiome compositions through the suppression  
129 of other microbes. Therefore, to determine the biological relevance of the observed bactericidal  
130 activity, we performed bacterial community analysis based on 16S ribosomal DNA profiling of tomato

131 and cotton root microbiomes following infection with wild-type *V. dahliae* or a *VdAve1* deletion  
132 mutant. Importantly, root microbiome compositions were determined during early *V. dahliae*  
133 infection stages, namely at ten days post inoculation when the fungus has just entered xylem vessels  
134 and initiated systemic spreading, to minimize indirect shifts in microbial compositions that result  
135 from severe disease symptomatology, rather than from direct shifts due to the presence of the  
136 effector protein. We did not observe major shifts in overall composition of bacterial phyla (Extended  
137 data Fig. 4a) or total microbial diversity ( $\alpha$ -diversity) (Extended data Fig. 4b) upon *V. dahliae*  
138 colonization of tomato and cotton. However, principal coordinate analysis based on Bray-Curtis  
139 dissimilarities ( $\beta$ -diversity) revealed a clear separation of root microbiomes (Fig. 2a) (PERMANOVA,  
140  $p < 0.01$  for both tomato and cotton). Importantly, the extent of *V. dahliae* colonization does not seem  
141 to determine the separation, as clustering of *V. dahliae* genotypes occurs in cotton although *VdAve1*  
142 deletion hardly affects fungal virulence on this host plant (Fig. 2a). Thus, as anticipated based on the  
143 potent, yet selective, antimicrobial activity, *VdAve1* secretion by *V. dahliae* sophisticatedly alters root  
144 microbiome compositions. Arguably, based on the sophisticated effects, a full and detailed  
145 characterization of microbiome composition changes requires large sample sizes and abundant  
146 numbers of repeats. However, strikingly, despite the relatively small sample size of our 16S rDNA  
147 profiling, pairwise bacterial order comparisons upon colonization by wild-type *V. dahliae* and the  
148 *VdAve1* deletion mutant revealed differential abundances of Sphingomonadales, Bdellovibrionales  
149 and Ktedonobacterales for tomato. (Fig. 2b) (Extended data Table 1). The finding that  
150 Sphingomonadales are repressed in the presence of *VdAve1* suggests that this taxon is the most  
151 sensitive to *VdAve1* activity. A similar comparison for cotton did not immediately reveal any  
152 differentially abundant orders, but agglomeration of amplicon sequence variants (ASVs) based on  
153 phylogenetic relatedness (patristic distance  $< 0.1$ ) revealed eight differentially abundant taxa,  
154 including a taxon of the Sphingomonadaceae family (Fig. 2b) (Extended data Table 2). Interestingly,  
155 although this taxon only represents a small proportion of all Sphingomonadaceae in the cotton root  
156 microbiomes, it is exclusively and consistently found in the microbiomes of roots infected by the

157 *VdAve1* deletion mutant, and completely absent upon infection with wild-type *V. dahliae*, again  
 158 pointing towards the particular sensitivity of this taxon towards *VdAve1*. Moreover, pairwise  
 159 comparisons following the combination of tomato and cotton samples based on infection by the  
 160 different *V. dahliae* genotypes, to identify differentially abundant bacterial orders that potentially  
 161 remained unnoticed due to the limited sample size, again only revealed differential abundance of



162 Sphingomonadales ( $p < 0.01$ ; Extended data Fig. 4c)(Extended data Table 3).

163

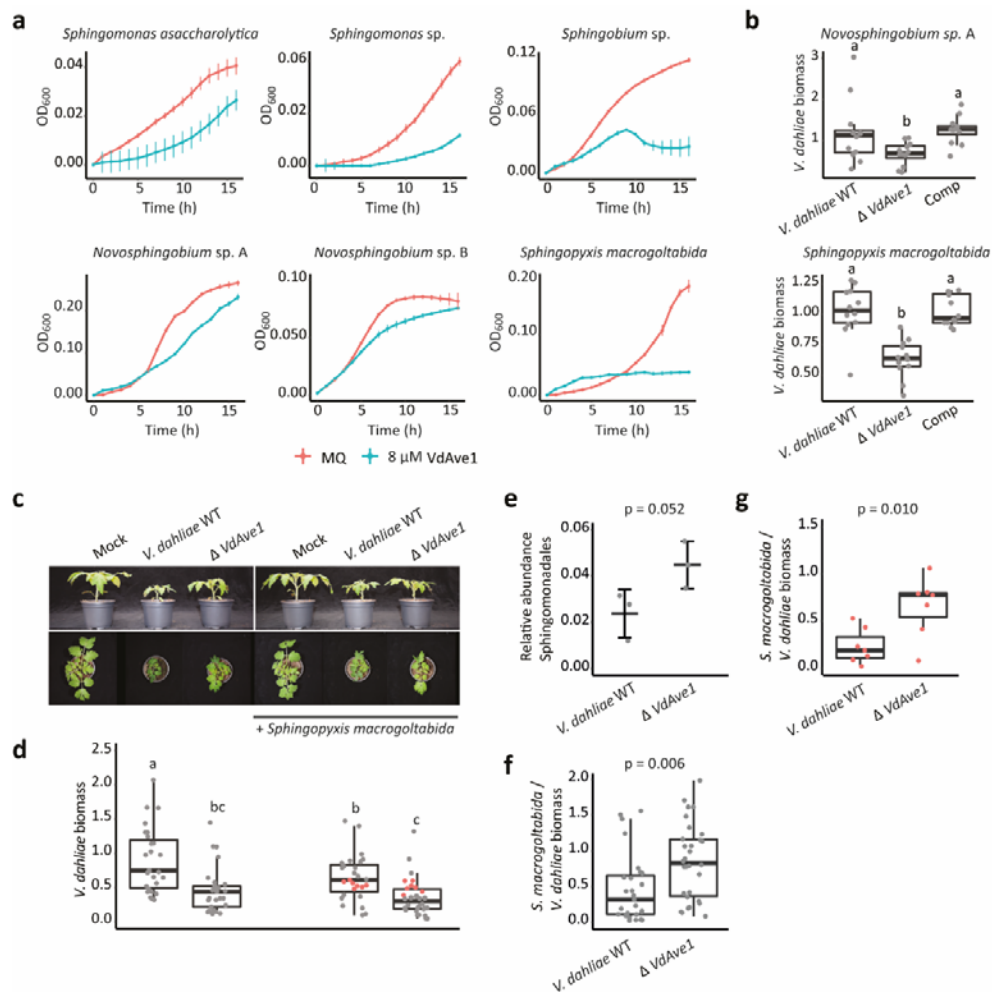
164 **Fig. 2: *Verticillium dahliae* VdAve1 impacts root microbiomes.** **a**, Principal coordinate analysis based  
 165 on Bray-Curtis dissimilarities reveals separation of root microbiome compositions ten days after  
 166 inoculation with wild-type *V. dahliae* and a *VdAve1* deletion mutant (PERMANOVA,  $p < 0.01$ ). **b**,  
 167 Differential abundance analysis of bacterial orders (tomato) and upon agglomeration of amplicon  
 168 sequence variants (patristic distance  $< 0.1$ ) (cotton) through pairwise comparison between root  
 169 microbiomes colonized by wild-type *V. dahliae* and a *VdAve1* deletion mutant (Wald test,  $p < 0.01$ ).  
 170 The average relative abundance (RA) of the differentially abundant taxa is indicated as a percentage  
 171 of the total bacterial community in the corresponding root microbiome. **c**, Sphingomonads  
 172 (*Sphingomonas*, *Novosphingobium*, *Sphingopyxis*, and *Sphingobium*) are repressed by *VdAve1*. Dots  
 173 represent single amplicon sequence variants with increased abundance (average of 3 samples) in



174 root microbiomes upon colonization by the *VdAve1* deletion mutant when compared with wild-type  
175 *V. dahliae*.

176 Given the fact that secretion of VdAve1 by *V. dahliae* during colonization of both tomato and cotton  
177 leads to a reduction of Sphingomonadales in the corresponding root microbiomes, we anticipated a  
178 broad efficacy of VdAve1 on bacteria within this order. Therefore, to identify Sphingomonadales  
179 genera that are most sensitive to VdAve1, we identified ASVs with increased average relative  
180 abundance in the microbiomes with the *VdAve1* deletion mutant when compared with wild-type *V.*  
181 *dahliae*, revealing *Sphingomonas*, *Novosphingobium*, *Sphingopyxis* and *Sphingobium* that are  
182 commonly referred to as Sphingomonads (Fig. 2c)<sup>22,23</sup>. To confirm that the reduced Sphingomonad  
183 abundance during *V. dahliae* colonization is a direct consequence of VdAve1 activity, we tested the  
184 sensitivity of a panel of plant-associated Sphingomonads to VdAve1 *in vitro*<sup>24,25</sup>. In accordance with  
185 the previously observed effect on *S. mali* (Fig. 1a), treatment with VdAve1 was found to also inhibit  
186 growth of *Sphingobium*, *Novosphingobium*, *Sphingopyxis* and two other *Sphingomonas* species (Fig.  
187 3a), indicating a broad sensitivity among the Sphingomonads. Given the selective efficacy of VdAve1  
188 and the strong effect on Sphingomonads in the tomato and cotton microbiomes, we hypothesized  
189 that these bacteria may act as antagonists and negatively affect *V. dahliae* growth in the absence of  
190 VdAve1. Indeed, co-cultivation of *V. dahliae* with *Novosphingobium* sp. A and *S. macrogoltabida*  
191 resulted in reduced fungal biomass for the *VdAve1* deletion mutant, when compared with the *V.*  
192 *dahliae* wild-type that secretes VdAve1 under these conditions, revealing that Sphingomonads  
193 comprise antagonists of *V. dahliae*, and explaining the importance of their inhibition by VdAve1 (Fig.  
194 3b). Accordingly, and in line with previously described observations of plant protective activities of  
195 Sphingomonad strains<sup>24</sup>, pre-treatment of surface-sterilized tomato seeds with *S. macrogoltabida*  
196 negatively affected Verticillium wilt disease development as confirmed through biomass  
197 quantification of wild-type *V. dahliae* in the presence and the absence of the bacterium (Fig. 3c,d)  
198 (Extended data Fig. 5). Importantly, quantification of *S. macrogoltabida* in the presence of wild-type  
199 *V. dahliae* and the *VdAve1* deletion mutant using 16S rDNA profiling and real-time PCR revealed that  
200 VdAve1 secretion significantly impacts *S. macrogoltabida* proliferation to counter its protective effect

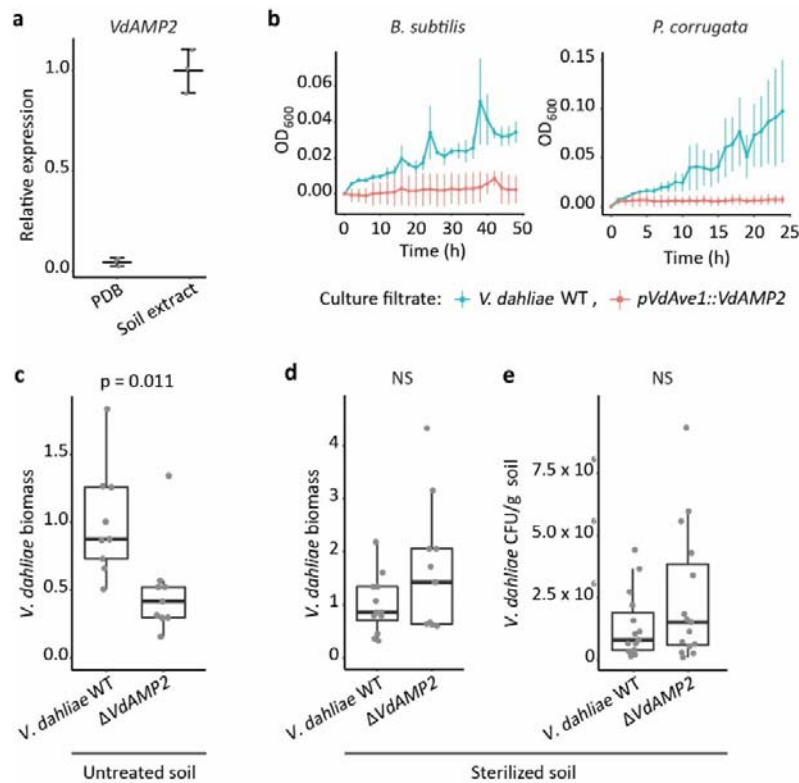
201 (Fig. 3e-g). Notably, this observation is not an indirect effect of differential host colonization by wild-  
 202 type *V. dahliae* and the *VdAve1* deletion mutant, as selection of tomato plants with equal levels of *V.*  
 203 *dahliae* biomass (Fig. 3d, data points highlighted in red), reveals similarly impaired *S. macrogoltabida*  
 204 proliferation in the presence of *VdAve1* (Fig. 3g). Thus, these data underpin the hypothesis that *V.*  
 205 *dahliae* secretes the *VdAve1* effector to target antagonistic bacteria, including Sphingomonadales,  
 206 during host colonization.



207 **Fig. 3: *Verticillium dahliae* VdAve1 affects antagonistic Sphingomonads.** **a**, Sphingomonads are  
 208 inhibited by VdAve1 in tomato xylem fluid. **b**, VdAve1 supports *V. dahliae* growth in the presence of  
 209 Sphingomonads. Biomass of wild-type *V. dahliae* (WT) and the *VdAve1* deletion ( $\Delta$ VdAve1) and  
 210 complementation (Comp) mutants was quantified following 48 hours of co-cultivation with  
 211 Sphingomonads in 0.5x MS medium (N=12). Letters represent significant differences (one-way  
 212 ANOVA and Tukey's post-hoc test;  $p < 0.05$  for *Novosphingobium* sp.;  $p < 0.0001$  for *S. macrogoltabida*).  
 213 **c**, Tomato seed treatment with *S. macrogoltabida* reduces Verticillium wilt symptoms (stunting; 14  
 214 days post inoculation). **d**, *V. dahliae* biomass in tomato stems determined with real-time PCR. Letters

215 represent significant biomass differences (one-way ANOVA and Tukey's post-hoc test;  $p < 0.05$ ;  $N \geq 27$ ).  
216 Each dot, grey or red, indicates the relative *V. dahliae* biomass in a single tomato plant. **e**, Relative  
217 abundance of Sphingomonadales according to 16S ribosomal DNA profiling of tomato plants pre-  
218 treated with *S. macrogoltabida* and infected with wild-type *V. dahliae* or the *VdAve1* deletion mutant  
219 (unpaired student's t-test;  $N=3$ ). **f**, Relative *Sphingopyxis* biomass in all pre-treated tomato plants  
220 infected with wild-type *V. dahliae* or the *VdAve1* deletion mutant, indicated by the grey and red dots  
221 in Fig. 3d combined, as quantified by real-time PCR (unpaired student's t-test;  $N \geq 27$ ). **g**, Relative  
222 *Sphingopyxis* biomass in pre-treated tomato plants colonized by similar amounts of wild-type *V.*  
223 *dahliae* or the *VdAve1* deletion mutant, indicated by the red dots in Fig. 3d, as quantified by real-time  
224 PCR (unpaired student's t-test;  $N=7$ ).

225 Our observation that *V. dahliae* secretes *VdAve1* to suppress microbial competitors in the  
226 microbiomes of its hosts, prompted us to speculate about additional *V. dahliae* effector proteins  
227 involved in microbiome manipulation. Based on our findings that canonical effector genes such as  
228 *VdAve1* can also be expressed outside the host, we hypothesized that *V. dahliae* also secretes  
229 effectors that aid in microbial competition in the soil. Therefore, to query for the occurrence of  
230 additional effectors that act in microbiome manipulation, the predicted secretome of *V. dahliae*  
231 strain JR2<sup>26</sup> was probed for structural homologs of known antimicrobial proteins (AMPs), revealing 10  
232 candidates (Extended data Table 4). The majority of the identified effectors share typical  
233 characteristics with canonical host-targeting effector proteins, such as being small and rich in  
234 cysteines. However, based on previously performed RNA sequencing experiments, no expression of  
235 any of these candidates could be monitored during colonization of *Arabidopsis thaliana*, *Nicotiana*  
236 *benthamiana* or cotton plants (Extended data Fig. 6)<sup>17,20,27,28</sup>. Additionally, *in vitro* cultivation of *V.*  
237 *dahliae* in the presence of *E. coli*, *B. subtilis* or *T. viride*, or of peptidoglycan to mimic bacterial  
238 encounter, did not lead to induction of any of the effector candidate genes (Extended data Fig. 6).  
239 Consequently, we hypothesized that these genes require other environmental triggers to be induced.  
240 Indeed, growth in soil extract consistently induced expression of candidate *VdAMP2* (Fig. 4a) that  
241 shares structural homology (confidence >90%) with amphipathic  $\beta$ -hairpins of aerolysin-type  $\beta$ -pore  
242 forming toxins ( $\beta$ -PFTs) (Extended data Fig. 7)<sup>29</sup>.



243

244 **Fig. 4: VdAMP2 contributes to *Verticillium dahliae* soil colonization.** a, *V. dahliae* VdAMP2 is  
245 induced after five days of cultivation in soil extract but not in potato dextrose broth (PDB). b, Growth  
246 of *B. subtilis* and *P. corrugata* in filter-sterilized culture filtrates from wild-type *V. dahliae* and the  
247 VdAMP2 expression transformant grown in liquid 0.2x PDB + 0.5x MS medium. c, VdAMP2  
248 contributes to soil colonization. *V. dahliae* biomass in soil samples was determined by real-time PCR  
249 seven days after inoculation with wild-type *V. dahliae* (WT) and the VdAMP2 deletion mutant  
250 ( $\Delta$ VdAMP2) (unpaired student's t-test; N=9). d,e VdAMP2 does not contribute to colonization in  
251 sterile soil. Experiment as shown in c in sterile soil. *V. dahliae* biomass was quantified with real-time  
252 PCR (N=9), d, and by colony forming unit counts per gram of soil (N=15), e.

253 To test for potential antimicrobial activity of VdAMP2, we attempted heterologous production of the  
254 effector protein. However, since production in *E. coli* and *Pichia pastoris* repeatedly failed,  
255 production in *V. dahliae* under control of the *VdAve1* promoter was pursued, resulting in high levels  
256 of VdAMP2 expression *in vitro* (Extended data Fig. 8a-c). Interestingly, proliferation of *B. subtilis* and  
257 of *P. corrugata* (Fig. 4b), but not of *F. oxysporum* and of *T. viride* (Extended data Fig. 9), was affected  
258 by filter-sterilized culture filtrate of the VdAMP2 expression transformant when compared with that  
259 of wild-type *V. dahliae*, suggesting that VdAMP2 exerts only antibacterial activity, like VdAve1 albeit  
260 with a different activity spectrum. Soil colonization assays using wild-type *V. dahliae* and a VdAMP2

261 deletion mutant (Extended data Fig. 8d-f) demonstrated that VdAMP2 contributes to *V. dahliae*  
262 fitness in the soil as measured by biomass accumulation (Fig. 4c). Importantly, since this fitness  
263 contribution is not observed in sterilized soil, we conclude that VdAMP2 contributes to *V. dahliae*  
264 fitness through its efficacy in microbial competition (Fig. 4d,e). As can be anticipated, the positive  
265 effect of VdAMP2 on biomass accumulation in the soil is reflected in disease development when  
266 plants are grown on this soil (Extended data Fig. 10), demonstrating that VdAMP2 positively  
267 contributes to virulence of *V. dahliae* in an indirect manner.

268 In conclusion, in this study we have demonstrated that *V. dahliae* employs effector proteins that  
269 contribute to niche colonization, during host-associated as well as during soil-dwelling stages,  
270 through the selective manipulation of local microbiomes. A wide array of microbially-secreted  
271 molecules has previously been described to fulfill crucial functions in intermicrobial competition,  
272 including hydrolytic enzymes, secondary metabolites and antimicrobial proteins. Some Gram-  
273 negative bacteria even employ a specialized type VI secretion system (T6SS) to translocate  
274 antimicrobial proteins into their microbial competitors<sup>30</sup>. In this manner, *Vibrio cholerae*, the causal  
275 agent of cholera, employs its T6SS to target members of the host commensal microbiota and hereby  
276 promotes colonization of the gut<sup>31</sup>. Similarly, the T6SS effector Hyde1 of the phytopathogen  
277 *Acidovorax citrulli* targets plant-associated bacteria *in vitro* and was speculated to play a role in  
278 microbial competition *in planta*<sup>7</sup>. This T6SS is analogous to the type III secretion system (T3SS) of  
279 Gram negative bacteria that acts as a needle-like structure to directly inject effector proteins into  
280 host cells to promote disease<sup>32</sup>. Similar secretion machinery intended for host-microbe or microbe-  
281 microbe interactions has not been described for fungi and other filamentous microbes, which instead  
282 secrete their effector proteins by extracellular deposition. Consequently, effector molecules targeted  
283 towards host cells or towards microbial competitors cannot be discriminated based on differential  
284 secretion motifs, such as those that determine type III versus type VI secretion in Gram negatives.  
285 Here, we have shown that the pool of effectors secreted by a fungal plant pathogen represents a  
286 diverse cocktail comprising proteins involved in the manipulation of the host as well as its

287 microbiome. Consequently, the effectors reported here likely only represent a small proportion of a  
288 larger subset of the *V. dahliae* effector repertoire that is intended for microbiome manipulation. For  
289 instance, similar effectors might be crucial during advanced infection stages to prevent secondary  
290 infections by opportunistic microbes when host defenses are impaired. Additionally, effector  
291 proteins can be anticipated to facilitate the survival of the *V. dahliae* resting structures that persist in  
292 the microbe-rich soil for years<sup>33</sup>. After all, possibly, fungal effectors with host microbiome-  
293 manipulating capacity initially evolved to limit bacterial growth in soil, as the advent of fungi on earth  
294 preceded land plant evolution and fungi initially likely co-evolved with bacteria in soil to compete for  
295 organic carbon. The discovery of further molecules for microbiome manipulation secreted by *V.*  
296 *dahliae* and other microbes, and unravelling of underlying modes of action, may ultimately lead to  
297 the development of novel antibiotics.

## 298 **Materials and methods**

299 All experiments have been repeated at least three times.

300 **Xylem fluid isolation.** Tomato plants (*Solanum lycopersicum* cv. MoneyMaker) were grown under  
301 controlled greenhouse conditions as described previously<sup>34</sup>. The stems of six-week-old plants were  
302 cut to allow oozing of the xylem fluid, which was collected on ice with a vacuum pump. The collected  
303 xylem fluid was centrifuged for 10 minutes at 20000 x g and filter-sterilized using a 0.2 µm filter  
304 (Sarstedt, Nümbrecht, Germany). The sterilized xylem fluid was stored at -20°C until use.

305 **Soil extract preparation.** To prepare soil extract, 100 grams of dry potting soil (Lentse potgrond,  
306 substraat arabidopsis, Lentse Potgrond BV, Katwijk, the Netherlands) was mixed with 500 mL of  
307 demineralized water and autoclaved for 15 minutes at 121°C. Soil particles were pelleted through  
308 centrifugation and the supernatant was collected and stored at -20°C until use.

309 **Gene expression analysis.** Total RNA of *V. dahliae* strain JR2 was isolated from tomato roots seven  
310 days after root dip inoculation and following five days of *in vitro* growth in soil extract and potato  
311 dextrose broth (PDB) using the Maxwell® 16 LEV Plant RNA Kit (Promega, Madison, USA). Real-time  
312 PCR was performed as described previously<sup>17</sup> to determine the expression of effector genes relative  
313 to *VdGAPDH* with primer pairs as shown in Extended data Table 6.

314 **Production and purification of recombinant effector proteins.** The sequences encoding mature  
315 VdAve1 and VnAve1 were cloned into pET-15b with an N-terminal His<sub>6</sub> tag sequence (Novagen,  
316 Madison, WI, USA) (primer sequences, see Extended data Table 6). The resulting expression vectors  
317 were confirmed by sequencing and used to transform *E. coli* strain BL21. For heterologous protein  
318 production, BL21 cells were grown in 1 x YT liquid medium at 37°C with constant shaking at 200 rpm.  
319 Protein production was induced with 1 mM IPTG final concentration when cultures reached an  
320 OD<sub>600</sub>=2 to ensure maximum yields. Following 2 hours of protein production, the bacterial cells were  
321 pelleted and snap-frozen in liquid nitrogen and then washed with 100 mM NaCl, 1 mM EDTA, and 10

322 mM Tris at pH 8.5. Cells were disrupted by stirring for 1 hour in lysis buffer (100 mM Tris, 150 mM  
323 NaCl, 10% glycerol, 6 mg/mL lysozyme (Sigma, St. Louis, MO, USA), 2 mg/mL deoxycholic acid, 0.06  
324 mg/mL DNaseI, protease inhibitor cocktail (Roche, Mannheim, Germany)) at 4°C. Soluble and  
325 insoluble fractions were separated by centrifuging at 20,000 x *g* for 10 min. The insoluble protein  
326 pellets were washed with 10 mL 1 M guanidine hydrochloride (GnHCl), 10 mM Tris at pH 8.0 and then  
327 denatured in 10 mL 6 M GnHCl, 10 mM β-mercaptoethanol, 10 mM Tris at pH 8.0. Samples were  
328 incubated for 1 hour at room temperature. Non-denatured debris was pelleted by centrifuging at  
329 20,000 x *g* for 10 min and discarded. Denaturation was allowed to continue for additional 3-4 hours.  
330 Proteins were purified under denaturing conditions by metal affinity chromatography using a column  
331 packed with 50% His60 Ni<sup>2+</sup> Superflow Resin (Clontech, Mountain View, CA, USA). The purified  
332 effector proteins were dialysed (Spectra/Por<sup>®</sup> 3 Dialysis Membrane, MWCO= 3.5 kDa) step-wise  
333 against 20 volumes of 0.25 M ammonium sulfate, 0.1 M BisTris, 10 mM reduced glutathione, 2 mM  
334 oxidized glutathione, pH 5.5 with decreasing GnHCl concentrations for refolding. Each dialysis step  
335 was allowed to proceed for at least 24 hours. Finally, proteins were dialysed against demineralized  
336 water. Final concentrations were determined using the BioRad Protein Assay (BioRad, Venendaal,  
337 The Netherlands).

338           Functionality of refolded VdAve1 was confirmed through recognition by the corresponding  
339 tomato immune receptor Ve1. To this end, an overnight culture of *A. tumefaciens* strain GV3101  
340 carrying the pSOL2092:Ve1 construct<sup>35</sup> was harvested by centrifugation and re-suspended to OD<sub>600</sub>=2  
341 in MMA (2% sucrose, 0.5% Murashige & Skoog salts (Duchefa Biochemie, Haarlem, The Netherlands),  
342 10 mM MES, 200 μM acetosyringone, pH 5.6) and infiltrated in the leaves of 5-week-old *N. tabacum*  
343 (cv. Petite Havana SR1) plants. After 24 hours, 10 μM of purified and refolded 6xHis-VdAve1 was  
344 infiltrated in leaf areas expressing Ve1. Photos were taken three days post infiltration of the effector  
345 protein.



346 **Generation of *V. dahliae* mutants.** To generate the *VdAMP2* effector deletion construct, *VdAMP2*  
347 flanking sequences were amplified using the primers listed in Extended data Table 6 and cloned into  
348 pRF-HU2<sup>36</sup>. To allow expression of *VdAMP2* under control of the *VdAve1* promoter, the coding  
349 sequence of *VdAMP2* was amplified and cloned into pFBT005. All constructs were transformed into  
350 *A. tumefaciens* strain AGL1 for *V. dahliae* transformation as described previously<sup>37</sup>.

351 ***V. dahliae* culture filtrates.** Conidiospores of *V. dahliae* strain JR2 and the *VdAMP2* expression  
352 transformant were harvested from potato dextrose agar (PDA) and diluted to a final concentration of  
353 10<sup>4</sup> conidiospores/mL in 20 mL of 0.2x PDB supplemented + 0.5x Murashige & Skoog medium  
354 (Duchefa, Haarlem, The Netherlands). Following four days of incubation at 22°C and 120 rpm, the  
355 fungal biomass was pelleted and the remaining supernatants were filter sterilized and stored at -20°C  
356 until use.

357 **Bacterial isolates.** Bacterial strains *Bacillus subtilis* AC95, *Staphylococcus xylosum* M3, *Pseudomonas*  
358 *corrugata* C26, *Streptomyces* sp. NE-P-8 and *Ralstonia* sp. M21 were obtained from our in house  
359 endophyte culture collection. Strains used in this study were all isolated from the xylem vessels of  
360 tomato cultivars from commercial greenhouses, both from stem and leaf sections. All strains were  
361 identified based on their 16S rRNA gene sequence using the primers 27F and 1492R (Extended data  
362 Table 6). 16S amplicons were sequenced by Sanger sequencing at Eurofins (Mix2Seq). The partial 16S  
363 rRNA gene sequences obtained were evaluated against the 16S ribosomal DNA sequence (Bacteria  
364 and Archaea) database from NCBI. Bacterial strains *Acidovorax* sp. (Leaf 73), *Arthrobacter* sp. (Leaf  
365 69), *Rhizobium* sp. (Leaf 167), *Serratia* sp. (Leaf 50), *Sphingomonas* sp. (Leaf 198), *Sphingobium* sp.  
366 (Leaf 26) and *Novosphingobium* sp. B (Leaf 2) were obtained from the At-SPHERE collection<sup>25</sup>.  
367 Bacterial strains *S. mali* (DSM 10565) and *S. asaccharolytica* (DSM 10564) were obtained from the  
368 DSMZ culture collection (Braunschweig, Germany). Bacterial strains *Novosphingobium* sp. A (NCCB  
369 100261), *S. macrogoltabida* (NCCB 95163), and *Sphingobacterium* sp. (NCCB 100093) were obtained  
370 from the Westerdijk Fungal Biodiversity Institute (Utrecht, The Netherlands).

371 ***In vitro* microbial growth assays.** Bacterial isolates were grown on lysogeny broth agar (LBA) or  
372 tryptone soya agar (TSA) at 28°C. Single colonies were selected and grown overnight at 28°C while  
373 shaking at 200 rpm. Overnight cultures were resuspended to OD<sub>600</sub>=0.05 in xylem fluid supplemented  
374 with purified effector proteins or diluted using culture filtrates to OD<sub>600</sub>=0.1. Additionally, *F.*  
375 *oxysporum* and *T. viride* spores were harvested from a PDA plate and suspended in xylem fluid  
376 supplemented with purified effector proteins or the *V. dahliae* culture filtrates to a final  
377 concentration of 10<sup>4</sup> spores/mL. 200 µL of the microbial suspensions was aliquoted in clear 96 well  
378 flat bottom polystyrene tissue culture plates. Plates were incubated in a CLARIOstar® plate reader  
379 (BMG LABTECH, Ortenberg, Germany) at 22°C with double orbital shaking every 15 minutes (10  
380 seconds at 300 rpm). The optical density was measured every 15 minutes at 600 nm.

381 **Scanning electron microscopy.** Samples for scanning electron microscopy were prepared as  
382 described previously with slight modifications<sup>38</sup>. In short, *B. subtilis* strain AC95 was grown overnight  
383 in LB and resuspended in xylem fluid to an OD<sub>600</sub>=0.05. Purified effector proteins were added to a  
384 final concentration of 6.5 µM (= 0.8 x MIC, VdAve1) and bacterial suspensions were incubated for 0,  
385 1, 3 and 7 hours. Next, 20 µL of the bacterial suspensions was transferred to poly-L-lysine coated  
386 glass slides (Corning, New York, USA) and incubated for another hour to allow binding of the  
387 bacteria. Glass slides were washed using sterile MQ and samples were fixed using 2.5%  
388 glutaraldehyde followed by postfixation in 1% osmium tetroxide. Samples were dehydrated using an  
389 ethanol dehydration series and subjected to critical point drying using a Leica CPD300 (Leica  
390 Mikrosysteme GmbH, Vienna, Austria). Finally, the samples were mounted on stubs, coated with  
391 12nm of tungsten and visualized in a field emission scanning electron microscope (Magellan 400, FEI,  
392 Eindhoven, the Netherlands).

393 **Root microbiome analysis.** Tomato and cotton inoculations were performed as described  
394 previously<sup>34</sup>. After ten days, plants were carefully uprooted and gently shaken to remove loosely  
395 adhering soil from the roots. Next, roots with rhizosphere soil from three tomato or two cotton

396 plants were pooled to form a single biological replicate. Samples were flash-frozen in liquid nitrogen  
397 and ground using mortar and pestle. Genomic DNA isolation was performed using the DNeasy  
398 PowerSoil Kit (Qiagen, Venlo, The Netherlands). Quality of the DNA samples was checked on a 1.0%  
399 agarose gel. Sequence libraries were prepared following amplification of the V4 region of the  
400 bacterial 16S rDNA (515F and 806R), and paired ends (250 bp) were sequenced using the HiSeq2500  
401 sequencing platform (Illumina, San Diego, USA) at the Beijing Genome Institute (BGI, Hong Kong,  
402 China).

403 Sequencing data was processed using R version 3.3.2. as described previously<sup>39</sup>. Briefly,  
404 amplicon sequence variants (ASVs) were inferred from quality filtered reads (Phred score >30) using  
405 the DADA2 method<sup>40</sup>. Taxonomy was assigned using the Ribosomal Database Project training set  
406 (RDP, version 16) and mitochondria- and chloroplast-assigned ASVs were removed. Next, ASV  
407 frequencies were transformed according to library size to determine relative abundances. The  
408 phyloseq package (version 1.22.3) was used to determine  $\alpha$ -diversity (Shannon index) and  $\beta$ -diversity  
409 (Bray-Curtis dissimilarity) as described previously<sup>33,41</sup>. Differential abundance analysis was performed  
410 using the DESeq2 extension within phyloseq<sup>42</sup>. To this end, a parametric model was applied to the  
411 data and a negative binomial Wald test was used to test for differential abundance of bacterial taxa  
412 with  $p < 0.01$  as significance threshold.

413 ***In vitro* competition assay.** Conidiospores of *V. dahliae* strain JR2 and the *VdAve1* deletion and  
414 complementation mutants were harvested from a PDA plate using sterile water and diluted to a final  
415 concentration of  $10^6$  conidiospores/mL in liquid 0.5x MS (Murashige and Skoog) medium (Duchefa,  
416 Haarlem, The Netherlands). Next, overnight cultures of *Novosphingobium* sp. and *S. macrogoltabida*  
417 were added to the conidiospores to  $OD_{600}=0.05$  and 500  $\mu$ L of the microbial suspensions was  
418 aliquoted in clear 12-well flat-bottom polystyrene tissue culture plates. Following 48 hours of  
419 incubation at room temperature, the microbial cultures were recovered and genomic DNA was  
420 isolated using the SmartExtract - DNA Extraction Kit (Eurogentec, Maastricht, The Netherlands). *V.*

421 *dahliae* biomass was quantified through real-time PCR using *V. dahliae* specific primers targeting the  
422 internal transcribed spacer (ITS) region of the ribosomal DNA (Extended data Table 6).

423 ***In planta* competition assay.** To allow *S. macrogoltabida* colonization of in the absence of other  
424 microbes, tomato seeds were incubated for five minutes in 2% sodium hypochlorite to ensure  
425 surface sterilization. Next, surface sterilized tomato seeds were washed three times using sterile  
426 water and transferred to a sterile Petri dish containing a filter paper pre-moistened with a *S.*  
427 *macrogoltabida* suspension in water ( $OD_{600}=0.05$ ). The tomato seeds were allowed to germinate *in*  
428 *vitro* and eventually transferred to regular potting soil, ten-day-old seedlings were inoculated as  
429 described previously<sup>34</sup>. Tomato stems were collected at 14 days post inoculation (dpi) and  
430 lyophilized prior to genomic DNA isolation with a CTAB-based extraction buffer (100 mM Tris-HCl pH  
431 8.0, 20 mM EDTA, 2 M NaCl, 3% CTAB). *V. dahliae* biomass was quantified with real-time PCR on the  
432 genomic DNA by targeting the internal transcribed spacer (ITS) region of the ribosomal DNA. The  
433 tomato *rubisco* gene was used for sample calibration. *S. macrogoltabida* biomass was quantified  
434 using *Sphingopyxis* specific primers (Extended data Table 6) and normalized using the *V. dahliae* ITS.  
435 Additionally, the relative abundance of the Sphingomonadales in three representative samples was  
436 determined by 16S ribosomal DNA profiling as described previously.

437 **Soil colonization assays.** Conidiospores of the *V. dahliae* strain JR2 and the mutants were harvested  
438 from PDA plate and a total of  $10^6$  conidiospores were added to 1 gram of potting soil. Samples were  
439 incubated at room temperature in the dark. After one week, DNA was extracted from the soil  
440 samples using the DNeasy PowerSoil Kit (QIAGEN, Venlo, The Netherlands). *V. dahliae* biomass was  
441 quantified through real-time PCR using *V. dahliae* specific primers targeting the internal transcribed  
442 spacer (ITS) region of the ribosomal DNA (Extended data Table 6). Primers targeting a conserved  
443 region of the bacterial 16S rRNA gene were used for sample equilibration.

444 To allow sample calibration when using sterilized potting soil (15 minutes at  
445 121°C), the samples were first mixed in a 1:1 ratio with fresh potting soil prior to DNA extraction.

446 Additionally, after one week of incubation of *V. dahliae* in the sterilized soil, serial dilutions were  
447 made and plated onto PDA to quantify colony forming units.

448 **Disease assays using *V. dahliae* microsclerotia.** *V. dahliae* microsclerotia were produced in a sterile  
449 moist medium of vermiculite and maize meal as described previously<sup>43</sup>. After four weeks of  
450 incubation, the vermiculite/microsclerotia mixture was dried at room temperature. Next, 150 mL of  
451 the dried mixture was mixed with 1 L of potting soil (Lentse potgrond, substraat arabidopsis, Lentse  
452 Potgrond BV, Katwijk The Netherlands) and Arabidopsis seeds of the Col-0 ecotype were sown at  
453 equal distances on top of the mixture. The above-ground parts of the plants were collected at 27 dpi  
454 and *V. dahliae* biomass was quantified through real-time PCR using *V. dahliae* specific primers  
455 targeting the internal transcribed spacer (ITS) region of the ribosomal DNA. The Arabidopsis *rubisco*  
456 gene was used for sample calibration (Extended data Table 6).

457 **References**

- 458 1 Rovenich, H., Boshoven, J. C. & Thomma, B. P. H. J. Filamentous pathogen effector functions:  
459 of pathogens, hosts and microbiomes. *Current opinion in plant biology* **20**, 96-103 (2014).
- 460 2 Stergiopoulos, I. & de Wit, P. J. Fungal effector proteins. *Annual Review of Phytopathology*  
461 **47**, 233-263 (2009).
- 462 3 Huttenhower, C. *et al.* Structure, function and diversity of the healthy human microbiome.  
463 *Nature* **486**, 207-214 (2012).
- 464 4 Turner, T. R., James, E. K. & Poole, P. S. The plant microbiome. *Genome Biology* **14**, 209  
465 (2013).
- 466 5 Bulgarelli, D. *et al.* Revealing structure and assembly cues for *Arabidopsis* root-inhabiting  
467 bacterial microbiota. *Nature* **488** 91-95 (2012).
- 468 6 Lundberg, D. S. *et al.* Defining the core *Arabidopsis thaliana* root microbiome. *Nature* **488**,  
469 86-90 (2012).
- 470 7 Levy, A. *et al.* Genomic features of bacterial adaptation to plants. *Nature Genetics* **50**, 138-  
471 150 (2017).
- 472 8 Koprivova, A. *et al.* Root-specific camalexin biosynthesis controls the plant growth-promoting  
473 effects of multiple bacterial strains. *PNAS* **116** (2019).
- 474 9 Huang, A. C. *et al.* A specialized metabolic network selectively modulates *Arabidopsis* root  
475 microbiota. *Science* **364** (2019).
- 476 10 Rudrappa, T., Czymmek, K. J., Pare, P. W. & Bais, H. P. Root-secreted malic acid recruits  
477 beneficial soil bacteria. *Plant physiology* **148**, 1547-1556 (2008).
- 478 11 Berendsen, R. L., Pieterse, C. M. & Bakker, P. A. The rhizosphere microbiome and plant  
479 health. *Trends in plant science* **17**, 478-486 (2012).
- 480 12 Berendsen, R. L. Disease-induced assemblage of a plant-beneficial bacterial consortium. *The*  
481 *ISME journal*, **12**, 1496- 1507 (2018)
- 482 13 Snelders, N. C., Kettles, G. J., Rudd, J. J. & Thomma, B. P. H. J. Plant pathogen effector  
483 proteins as manipulators of host microbiomes? *Molecular plant pathology* **19**, 257-259  
484 (2018).
- 485 14 Fradin, E. F. & Thomma, B. P. H. J. Physiology and molecular aspects of *Verticillium* Wilt  
486 diseases caused by *V. dahliae* and *V. albo-atrum*. *Molecular plant pathology* **7**, 71-86 (2006).
- 487 15 Klosterman, S. J., Atallah, Z. K., Vallad, G. E. & Subbarao, K. V. Diversity, pathogenicity, and  
488 management of *Verticillium* species. *Annual Review of Phytopathology* **47**, 39-62 (2009).
- 489 16 Mol, L. & Van Riessen, H. Effect of plant roots on the germination of microsclerotia of  
490 *Verticillium dahliae*. *European journal of plant pathology* **101**, 673-678 (1995).
- 491 17 de Jonge, R. *et al.* Tomato immune receptor Ve1 recognizes effector of multiple fungal  
492 pathogens uncovered by genome and RNA sequencing. *PNAS* **109**, 5110-5115 (2012).
- 493 18 Ficarra, F. A., Grandellis, C., Garavaglia, B. S., Gottig, N. & Ottado, J. Bacterial and plant  
494 natriuretic peptides improve plant defence responses against pathogens. *Molecular plant*  
495 *pathology* **19**, 801-811 (2018).
- 496 19 Gehring, C. A. & Irving, H. R. Natriuretic peptides - a class of heterologous molecules in  
497 plants. *International Journal of Biochemistry & Cell Biology* **35**, 1318-1322 (2003).
- 498 20 Faino, L., de Jonge, R. & Thomma, B. P. H. J. The transcriptome of *Verticillium dahliae*-  
499 infected *Nicotiana benthamiana* determined by deep RNA sequencing. *Plant Signaling &*  
500 *Behavior* **7**, 1065-1069 (2012).
- 501 21 Ingham, A. B. & Moore, R. J. Recombinant production of antimicrobial peptides in  
502 heterologous microbial systems. *Biotechnology and Applied Biochemistry* **47**, 1-9 (2007).
- 503 22 Takeuchi, M., Hamana, K. & Hiraiishi, A. Proposal of the genus *Sphingomonas* sensu stricto  
504 and three new genera, *Sphingobium*, *Novosphingobium* and *Sphingopyxis*, on the basis of

- 505 phylogenetic and chemotaxonomic analyses. *International Journal of Systematic and*  
506 *Evolutionary Microbiology* **51**, 1405-1417 (2001).
- 507 23 Aylward, F. O. *et al.* Comparison of 26 Sphingomonad genomes reveals diverse  
508 environmental adaptations and biodegradative capabilities. *Applied and Environmental*  
509 *Microbiology* **79**, 3724-3733 (2013).
- 510 24 Innerebner, G., Knief, C. & Vorholt, J. A. Protection of *Arabidopsis thaliana* against leaf-  
511 pathogenic *Pseudomonas syringae* by *Sphingomonas* strains in a controlled model system.  
512 *Applied and Environmental Microbiology* **77**, 3202-3210 (2011).
- 513 25 Bai, Y. *et al.* Functional overlap of the *Arabidopsis* leaf and root microbiota. *Nature* **528**, 364-  
514 369 (2015).
- 515 26 Faino, L. *et al.* Single-molecule real-time sequencing combined with optical mapping yields  
516 completely finished fungal genome. *mBio* **6** (2015).
- 517 27 Depotter, J. R. L. *et al.* Homogenization of sub-genome secretome gene expression patterns  
518 in the allodiploid fungus *Verticillium longisporum*. Preprint at  
519 <https://www.biorxiv.org/content/10.1101/341636v1> (2018).
- 520 28 Gibriel, H., Li, J., Zhu, L., Seidl, M. & Thomma, B. P. H. J. *Verticillium dahliae* strains that infect  
521 the same host plant display highly divergent effector catalogs. Preprint at  
522 <https://www.biorxiv.org/content/10.1101/528729v1> (2019).
- 523 29 Dal Peraro, M. & van der Goot, F. G. Pore-forming toxins: ancient, but never really out of  
524 fashion. *Nature Reviews Microbiology* **14**, 77-92 (2016).
- 525 30 Coulthurst, S. The Type VI secretion system: a versatile bacterial weapon. *Microbiology* **165**,  
526 503-515 (2019).
- 527 31 Zhao, W., Caro, F., Robins, W. & Mekalanos, J. J. Antagonism toward the intestinal microbiota  
528 and its effect on *Vibrio cholerae* virulence. *Science* **359**, 210-213 (2018).
- 529 32 Alfano, J. R. & Collmer, A. Type III secretion system effector proteins: double agents in  
530 bacterial disease and plant defense. *Annual Review of Phytopathology* **42**, 385-414 (2004).
- 531 33 Xiong, D. *et al.* Deep mRNA sequencing reveals stage-specific transcriptome alterations  
532 during microsclerotia development in the smoke tree vascular wilt pathogen, *Verticillium*  
533 *dahliae*. *BMC Genomics* **15**, 324, (2014).
- 534 34 Fradin, E. F. *et al.* Genetic dissection of *Verticillium* Wilt resistance mediated by tomato Ve1.  
535 *Plant physiology* **150**, 320-332 (2009).
- 536 35 Zhang, Z. *et al.* Optimized agroinfiltration and virus-induced gene silencing to study Ve1-  
537 mediated *Verticillium* resistance in tobacco. *Molecular Plant Microbe Interactions* **26**, 182-  
538 190, (2013).
- 539 36 Frandsen, R. J., Andersson, J. A., Kristensen, M. B. & Giese, H. Efficient four fragment cloning  
540 for the construction of vectors for targeted gene replacement in filamentous fungi. *BMC*  
541 *Molecular Biology* **9**, 70 (2008).
- 542 37 Santhanam, P. in *Plant Fungal Pathogens* 509-517 (Springer, 2012).
- 543 38 Bozzola, J. J. Conventional specimen preparation techniques for scanning electron  
544 microscopy of biological specimens. *Methods in Molecular Biology* **1117**, 133-150 (2014).
- 545 39 Callahan, B. J., Sankaran, K., Fukuyama, J. A., McMurdie, P. J. & Holmes, S. P. Bioconductor  
546 Workflow for Microbiome Data Analysis: from raw reads to community analyses.  
547 *F1000Research* **5**, 1492 (2016).
- 548 40 Callahan, B. J. *et al.* DADA2: High-resolution sample inference from Illumina amplicon data.  
549 *Nature Methods* **13**, 581, (2016).
- 550 41 McMurdie, P. J. & Holmes, S. phyloseq: an R package for reproducible interactive analysis  
551 and graphics of microbiome census data. *Plos One* **8**, e61217 (2013).
- 552 42 Love, M. I., Huber, W. & Anders, S. Moderated estimation of fold change and dispersion for  
553 RNA-seq data with DESeq2. *Genome Biology* **15**, (2014).

554 43 Depotter, J. R. L., Thomma, B. P. H. J. & Wood, T. A. Measuring the impact of *Verticillium*  
555 *longisporum* on oilseed rape (*Brassica napus*) yield in field trials in the United Kingdom.  
556 *European Journal of Plant Pathology* **153**, 321-326 (2019).  
557 44 de Jonge, R. *et al.* Extensive chromosomal reshuffling drives evolution of virulence in an  
558 asexual pathogen. *Genome Research* **23**, 1271-1282 (2013).  
559 45 Kelley, L. A. *et al.* The Phyre2 web portal for protein modeling, prediction and analysis.  
560 *Nature protocols*, **10**, 845-858 (2015)

561

562 **Acknowledgments:** The authors thank M. Giesbers from the Wageningen Electron Microscopy  
563 Centre for technical assistance. Work in the laboratory of B.P.H.J.T is supported by the Research  
564 Council Earth and Life Sciences (ALW) of the Netherlands Organization of Scientific Research (NWO).

565 **Author contributions:** N.C.S., H.R. and B.P.H.J.T. conceived the project. N.C.S., H.R., G.C.P., J.R.M. and  
566 B.P.H.J.T. designed the experiments. N.C.S., H.R., G.C.P., M.R.F., M.F.S. and R.N. carried out the  
567 experiments, N.C.S., H.R., G.C.P., M.R.F., M.F.S., J.A.V., R.N., J.R.M. and B.P.H.J.T. analysed the data.  
568 N.C.S. and B.P.H.J.T. wrote the manuscript. All authors read and approved the final manuscript.

569 **Competing interests:** Authors declare no competing interests.

570 **Data and materials availability:** The metagenomics data have been deposited in the European  
571 Nucleotide Archive (ENA) under accession number PRJEB34281.